Electronic Supplementary Information (ESI)

Laser synthesized super-hydrophobic conducting carbon with broccoli-type morphology as a counter-electrode for dye sensitized solar cells

Rohan Gokhale,[a] Shruti Agarkar,[a] Joyashish Debgupta,[a] Deodatta Shinde,[b] Benoit Lefez,[c] Abhik Banerjee,[a] Jyoti Jog,[a] Mahendra More,[b] Beatrice Hannoyer,[c] and Satishchandra Ogale[a]*

[a] National Chemical Laboratory, Council of Scientific and Industrial Research, Dr Homi Bhabha Road, Pune 411008, India.

[b] Centre for Advanced Studies in Materials Science and Condensed Matter Physics, Department of Physics, University of Pune, Pune 411008, India.

[c] *Universit´e de Rouen, GPM UMR 6634 CNRS – BP 12, 76801, Etienne du Rouvray Cedex, France.*

ESI-I

Materials and Equipment:

High purity (GR grade) routine organic solvent o-Dichlorobenzene (DCB) were obtained from Merck Chemicals and were used as received. A 248 nm KrF excimer laser (Lambda Physic – Germany) with a maximum average power of 40 watts (pulse energy = 150 mJ) and a pulse-width of 20 ns was used in the irradiation process. Field Emission Scanning Electron Microscopy (FESEM, Hitachi S-4200) was used for obtaining the images. Raman spectroscopy (a confocal micro-Raman spectrometer LabRAM ARAMIS Horiba JobinYvon, with laser excitation wavelength of 532 nm) was used to examine the characteristics of the carbon films. Thermogravimetric analysis (TGA) was performed to determine the thermal stability. Scanning electron microscopy (FEI Quanta 200 3D) was also used for the determination of morphology. Sheet Resistance of the Films was measured on a Four-Probe system.

Fabrication of Solar Cells: DSSC solar cells were made using doctor blading method using the commercially available P25 nanopowder (TiO_2). After making the films they were annealed at 450^{o}C for 60 min., the films were dipped in Ruthenium N719 dye for sensitization for 24 h at room temperature. The samples were then rinsed with ethanol to remove excess dye on the surface and air-dried at room temperature. This was followed by redox electrolyte addition and top contact of Pt coated FTO or carbon counter electrode. The electrolyte used was 0.6M 1-propyl-2, 3-dimethyl-imidazolium iodide, 0.1 M LiI, 0.05 M I_2, and 0.5 M 4-tert butylpyridine in acetonitrile/valeronitrile solution (v/v 1:1).

Electrolyte spreading time measurement: The spreading time of the liquid (electrolyte) on the surface was measured by recording series of images (with 40 msec interval between two successive images) from the time of contact of liquid droplet with the substrate with a CCD camera attached with the Digidrop contact angle meter. Later, each image was analyzed using WinDrop software to get the contact angle values with time. This was done until the contact angle value reached zero, i.e., complete spreading. Care was taken to minimize the error due to evaporation of the liquid during recording. This gave the time of spreading of the electrolyte for each substrate.

ESI-II

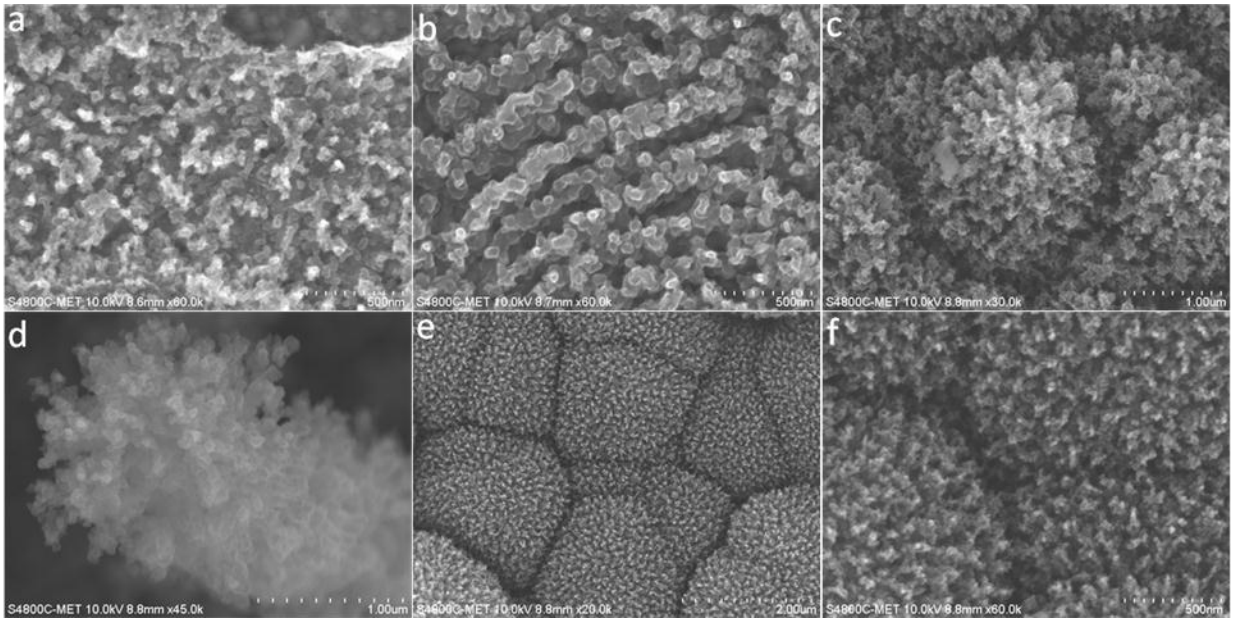

Fig S1. FESEM images of the carbon films during growth. Evidence of assembly of carbon nanoparticles (a) 15 seconds (b) 30 seconds (c-d) 3 min (e-f) 5 min

ESI- III

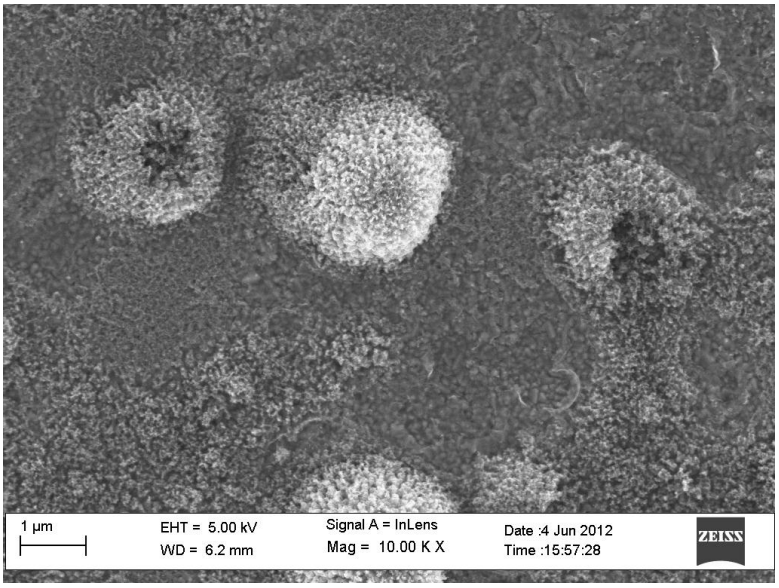

Fig S2. *Ruptured peaks in the 15 mins irradiated system*

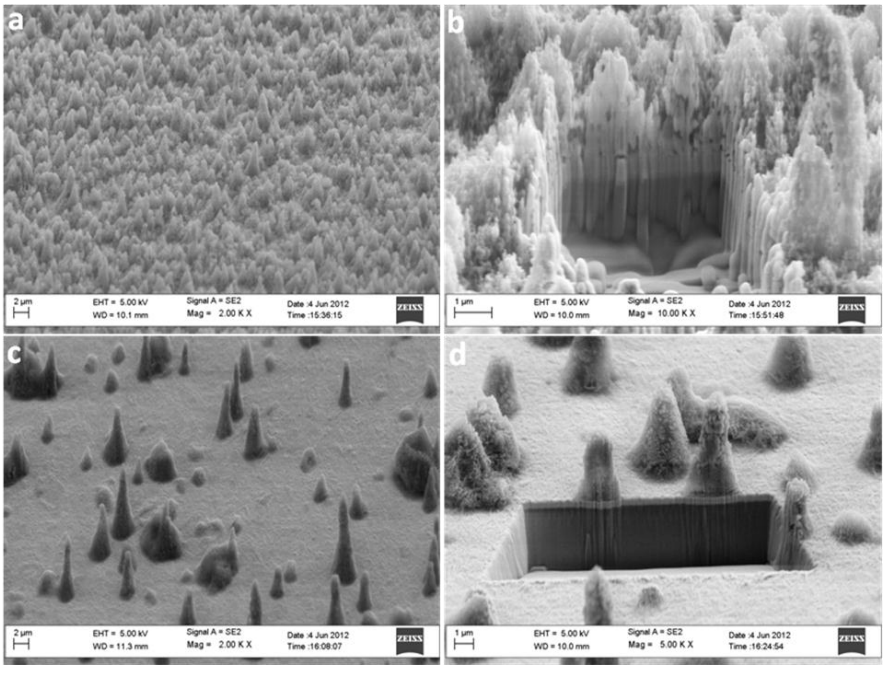

Figure S3. *Cross section FE SEM images of the obtained for (a-b) 3 mins film (c-d) 15 mins film*

Continued irradiation beyond 5 minutes leads to gradual changes in the morphology of the carbon structures which yield some interesting results as far as the application study is concerned. It is observed that exposure of the carbon film to excessive laser photons beyond the 15 minutes window studied in this work, results in total loss of carbon by laser ablation. Once the reactant molecules completely form carbon nanostructures by the photochemical stitching process which we have described, additional UV photons continue to strike the carbon material. The laser induced heat causes carbon loss by ablation of the target. The carbon film becomes more porous, accessible, accompanied by a decreasing film thickness. As is visible from **Fig S3** the carbon broccoli structures formed up to 5 minutes gradually becomes less dense with more exposure to UV photons. **Fig S3 c-d** show the case of the 15 minutes laser irradiated carbon film which demonstrates a much less dense film as compared to the 3 minutes case (**Fig S3-b**). This structural change also leads to a significant decrease in the surface roughness leading to a less hydrophobic character as discussed later. The SEM images of the 15 minutes case also reveals systemic ruptures in the vertically aligned forests due to excessive laser treatment (Fig S2).

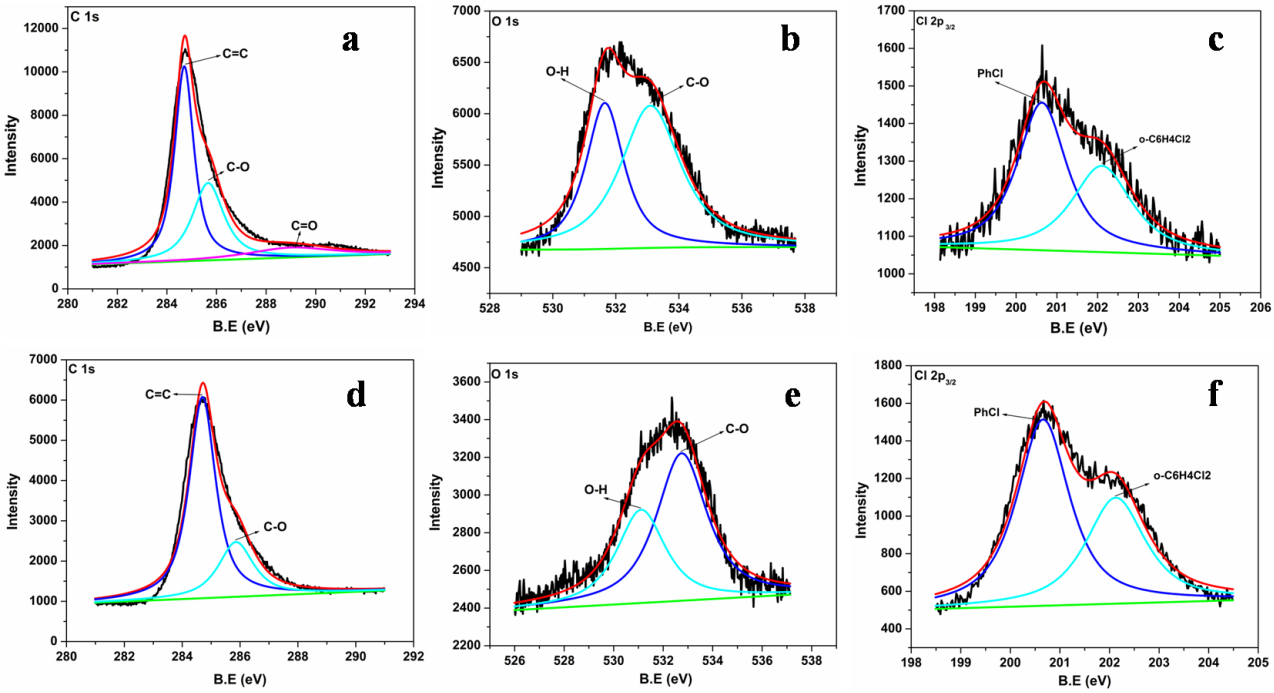

Figure S4. (a-c). XPS spectra for the 3 mins case of laser carbon film (d-f). XPS spectra for the 15 mins laser carbon film. **a.** C1s **b.** O1s **c.** Cl $2p_{3/2}$ **d.** C1s **e.** O1s **f.** Cl $2p_{3/2}$

We carried out the X-ray photoelectron spectroscopy (XPS) of two cases of carbon films, the 3 min case and the best performing 15 minutes case. It was observed that the carbon material in both cases contained the elements, carbon, oxygen and residual chlorine. The carbon in both the films existed in sp^2 C=C form and the C-O form. Similarly there was also considerable oxygen content in both the films. The C-Cl bonds detected in the XPS of these films, probably arises due to residual content from the halogen containing reactant.

The Tables T1 and T2 give the calculated atomic percentage of C, O and Cl from the XPS of both the carbon films.

Table T1 (3 min film)

Element	Atomic percentage
C	**64.15**
O	**30.84**
Cl	**4.99**

Table T2 (15 min film)

Element	Atomic percentage
C	**60.41**
O	**33.89**
Cl	**5.69**

From the XPS data, it was thus clearly observed that the 15 minutes laser irradiated case showed a greater percentage of oxygen content than the 3 minute case. The percentage of residual Chlorine was observed to be similar in both cases.

This data can also provide a suitable explanation for a systematically increasing efficiency. As the oxygen content gradually increases, the number of catalytic sites also increase in the counter-electrode resulting in a greater performance with increasing time of irradiation.

ESI-IV

Electronic properties of the carbon films

Measurements for electronic conductivity of all the carbon film cases were done by a two probe system using a probe station. Each film case was prepared on a non-conducting glass surface. Contacts at the two ends of the film in each case were obtained with the help of a conducting Aluminum tape. Current voltage curves were obtained across these films with Al contacts. The carbon I-V showed an ohmic behavior. The following table (Table 3) shows the observed and further calculated values for the electronic nature of these carbon films.

Film	Approximate Thickness (nm)	Resistance (Ω)	Conductivity *10^2 ($S.m^{-1}$)	Resistivity *10^-2 (Ω.m)
15 sec	155	709220	0.13	7.70
1 min	510	7485	3.75	0.27
3 min	4750	826	3.63	0.28
5 min	4750	558.6	5.40	0.19
10 min	4750	390.6	7.69	0.13
15 min	4750	1483.6	2.03	0.49

Table 3. *Electronic properties of the carbon films.*

The length of the film in each case was maintained at a constant value of l=1 cm =0.01 m

Conductivity calculation was done by the following way:

$R=\sigma l/A$; $\sigma= RA/l$; where σ is the resistivity, R is the resistance, l is the length of the film and A is the area of cross section of the conductor.

A= thickness of the film* width of the film; width in each case was a constant of 0.7 cm

It is clearly observed that the conductivity values gradually increase with time for the carbon films prepared. This also reflects in the correspondingly increasing efficiency of the solar cells. The resistance for the 15 seconds film is very high because of the incomplete formation of the carbon film. The conductivity for the 1 min and 3 min case is nearly similar. The 5 min and 10 minutes cases show a further decreased resistance. Interestingly, the highest efficiency case (15 mins) however shows a decrease in conductivity. This may occur due to a decreased carbon content due to gradual ablation and more number of oxidized sites due to large exposure time to UV-photons. The efficiency however is high because of the larger porosity of the film and a more number of catalytic sites.

The sheet resistance (Table T4) of some cases (on non-conducting glass surface) obtained with a four-probe system also confirms a similar trend in the electronic properties of these carbon systems.

Carbon Film	**Sheet Resistance (kΩ/□)**
3 min	2.63
5 min	1.33
15 min	10.24

Table T4. *Sheet Resistance of the pure carbon films*

ESI-V

The surface energies of the 3 min and 5 min films are calculated according to Wu's method[a] using three different liquids (DMSO, Ethylene glycol and Glycerol). The calculation shows an increase in the surface energy from 3 min to 5 min irradiated film (44.8 mN/m to 47.1 mN/m, respectively). This surface energy is composed of two components namely dispersive or non-polar component and a polar component. The polar component of surface energy increases from 3 min to 5 min film (14 mN/m to 18 mN/m) whereas dispersive component decreases slightly (30.7 mN/m to 29.2 mN/m). This means that the 5 min film has more hydrophilic character than that of 3 min film. This fact is in accordance with the lower contact angle value for the 5 min film as compared to the 3 min film. Moreover, the enhanced polar character binds the water droplet on the surface and results in higher sliding angle for the 5 min film. When the film reaches a less hydrophobic state (eg. the 15 minute case) the hydrophobicity can be reset to higher values as shown in **Figure 4**. This can be done by adding 1-2 drops of additional DCB and re-irradiating the film for a period for 3 minutes. The contact angle suddenly increases to 142 ± 2^{o}. This process can be repeated again for achieving a higher contact angle. This laser induced tunability of the hydrophobicity of carbon films is certainly an interesting scientific realm.

ESI-VI

Cyclic Voltammetry

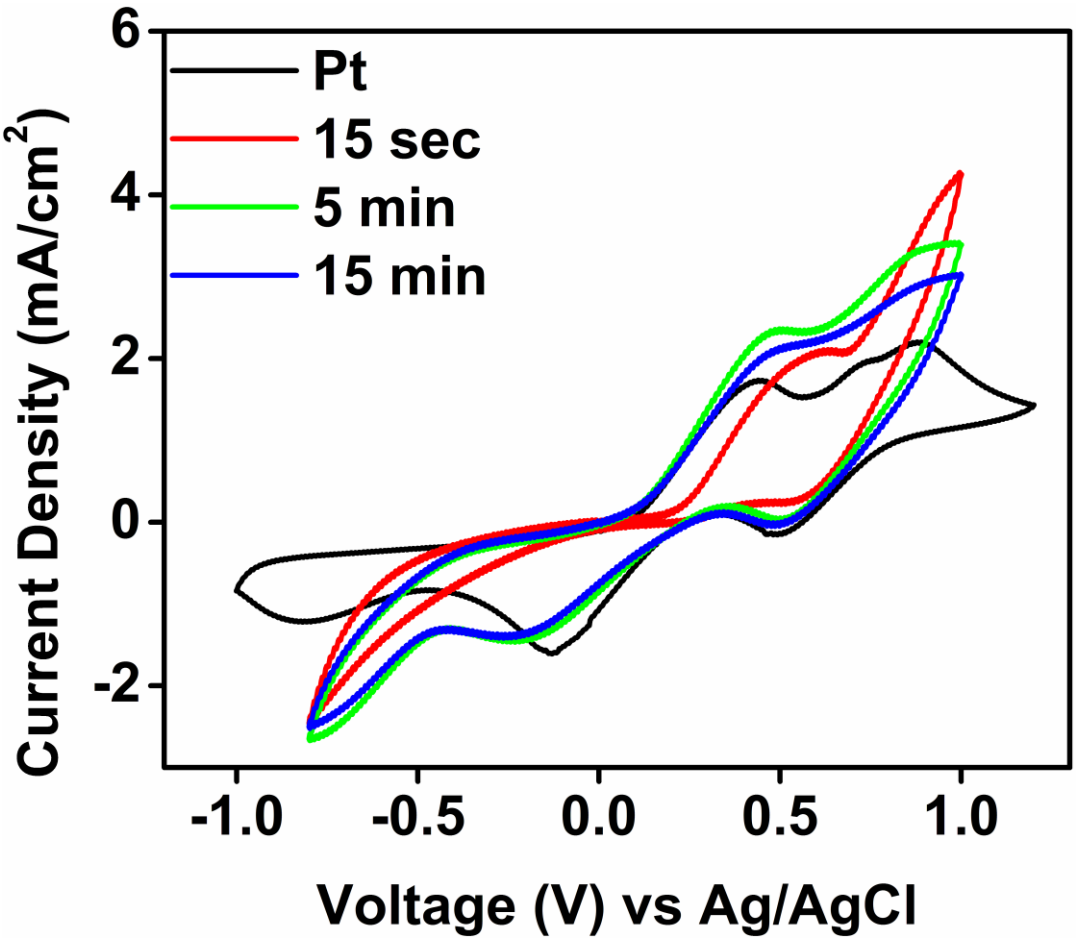

Area of the electrodes used =0.5 cm^2

Fig S5. *Cyclic Voltametry studies of Pt and various carbon electrodes.*

Electrochemical stability

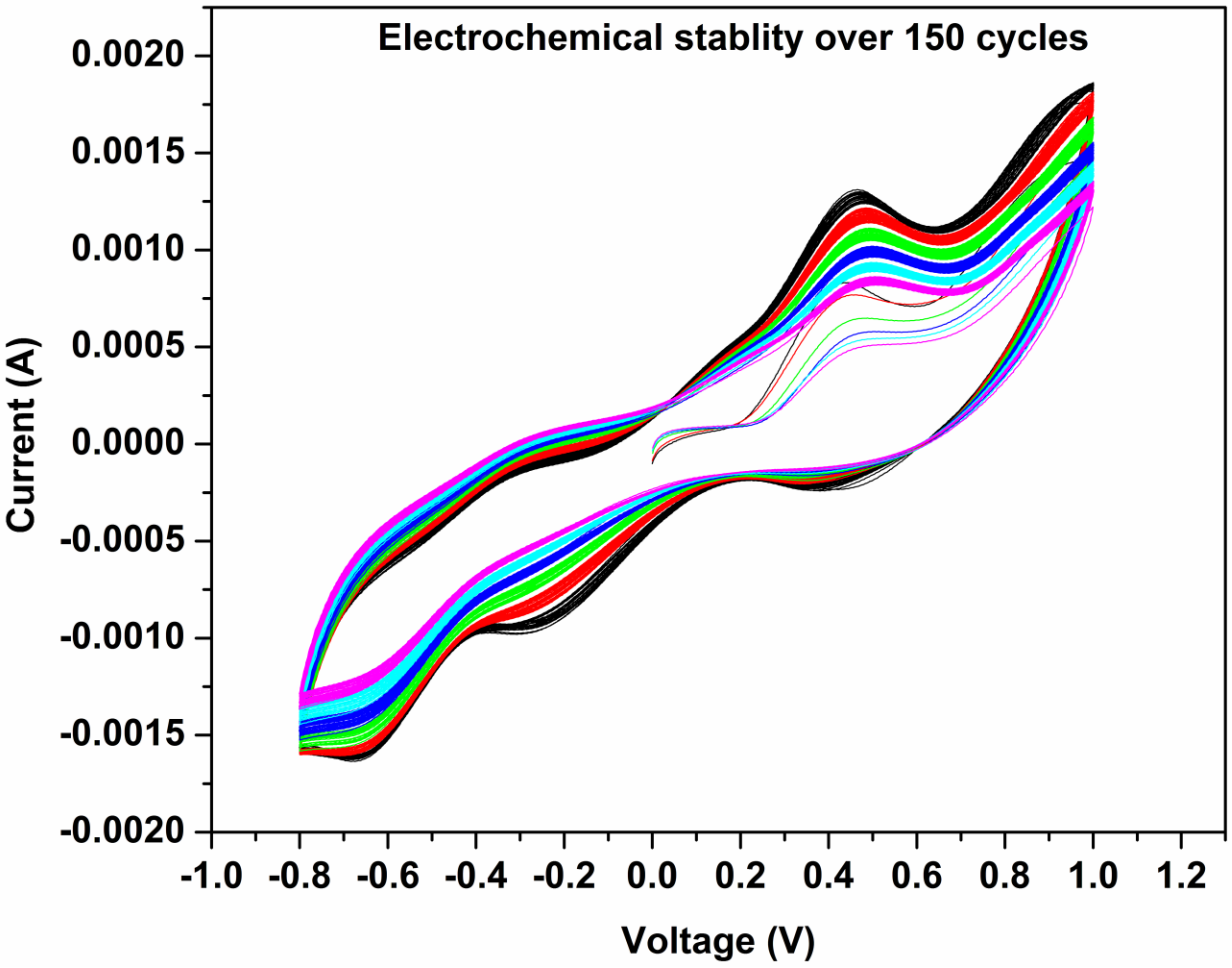

Fig S6. *Electrochemical stability of the 15 min laser formed electrode over 150 cycles*

ESI-VII

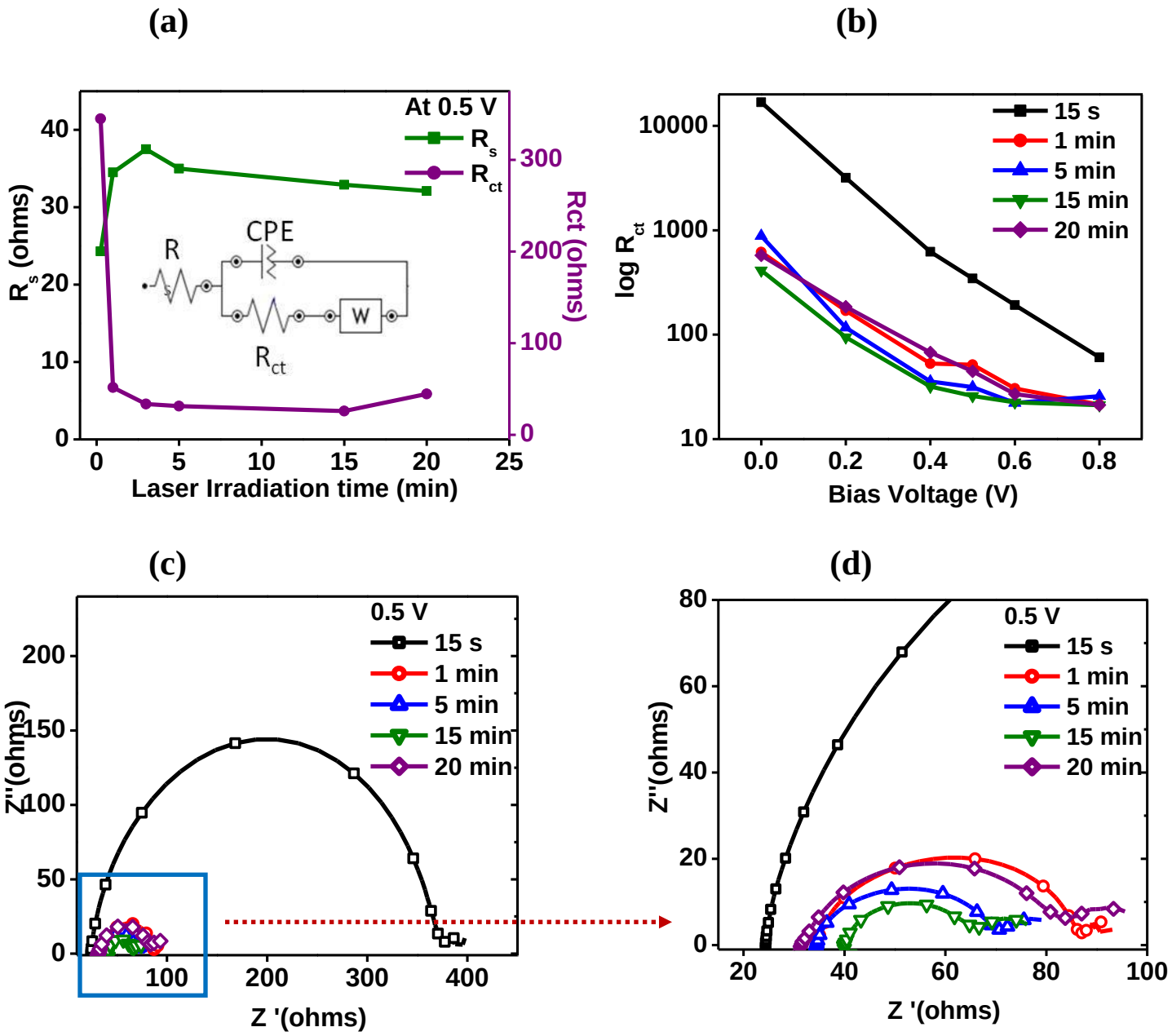

Figure S7 *a) Plot of Rs and Rct vs Laser irradiation time b) Plot of Log Rct vs bias voltage for 15 s, 1min , 5 min , 10 min and 20 min laser formed Counter electrode c) Nyquist plots for various C counter electrodes as bias voltage 0.5V d) zoomed version of (c)*

Impedance measurements were performed to determine the catalytic charge transfer resistance of all carbon counter electrodes. A Symmetric cell assembly was used to perform this measurement[b]. The electrochemical cell consisted of two identical carbon counter electrodes with area 0.5 cm^2 each placed in a flip chip assembly. The space between the electrodes was filled with liquid electrolyte consisting of 0.5M LiI and 0.05 M I_2. The frequency range selected for the measurement was 0.1 Hz to 1 MHz with AC amplitude of 10 mV. Nyquist plots were obtained for all carbon counter electrodes by applying bias voltage varying from 0V to 0.8V. Nova 1.7 software was used to fit the above Nyquist plots. Figure S7a shows plot of R_s and R_{ct} versus laser irradiation time and inset is the equivalent circuit used to fit the Nyquist plots. Figure S5b shows the plot of log R_{ct} versus applied voltage for different laser formed counter electrodes. R_s, which is the serial ohmic resistance which reflects the adhesion of carbon film on substrate is between 25-35 Ω for all laser formed counter electrodes. This indicates that all laser formed counter electrodes have fairly good adhesion with the substrate. All the laser formed films follow proper trend where R_{ct} decreases with increase in applied bias voltage and the Nernst diffusion impedance starts increasing as seen in figure S7 b. From the figure S7 a and b it is seen that catalytic charge transfer resistance, R_{ct} decreases with irradiation time and is lowest for 15 min laser formed film. It shows an increase for 20 min laser irradiated case. This matches well with the high efficiency performance of 15 min laser formed counter electrode compared to the other laser formed counter electrodes. 15 min laser formed counter electrode has shows good catalytic activity and better charge transfer properties at the electrode electrolyte interface. Figure S7c-d shows Nyquist plots of 15 min laser formed counter electrodes at different bias voltage.

ESI-VIII

Adhesion test of the films

The carbon films are prepared by a room temperature, binder free process and not subjected to any thermal post treatment. Considering these parameters, the adhesion of the films onto FTO-glass is quite good. The films do not peel of easily. In fact, we tested the adhesion by sticking a scotch tape on the surface of the film and removing it. As can be seen from the figure below, the amount of carbon removed by the scotch tape is negligible except at the very edges, highlighting the good adhesion of these laser prepared carbon films.

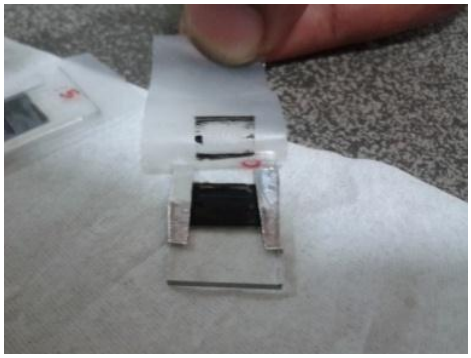

Scotch tape after complete removal

ESI-IX

Field Emission Studies:

Electron sources are the chief building blocks of various applications such as flat panel displays, x-ray sources, mass spectrometers and space based applications like thrusters, tethers etc. In all these applications thermionic emitters have been replaced by the field emitters. This has become possible because of the current developments of cheap and robust field emitters. The ideal field emitter should possess high aspect ratio, and good conductivity material with high mechanical strength, in addition to being robust, cheap and easy to process. Carbon based materials like CNT [d], Graphene [e], and Diamond [f] have already demonstrated their ability to become potential candidates as field emitters. In this work we studied the field emission (FE) behavior of three different specimens viz, 3 minute laser irradiated film (Specimen A), 5 minute laser irradiated film (Specimen B) and a rather interesting case of a thin layer graphene drop-cast on the 3 minute laser irradiated carbon film (Specimen C). The field emission current density-electric field (J-E) characteristics were obtained in all-metal field emission microscope with load-lock chamber in ultra high vacuum (UHV) conditions. The experimental procedures for current density measurements are described in detail elsewhere [g]. In this study, the effective emission area was ~0.25 cm^2 and cathode to anode distance was kept ~500 µm for all the specimen.

Figure S8 (a) depicts the field emission current density as a function of applied electric field (J-E). The turn-on field, defined as the field required to draw an emission current of ~ 10 $\mu A/cm^2$, is found to be ~ 9 V/µm, 7.5 V/µm and 5.6 V/µm for Specimen A, B and C respectively. The results are summarized in Table 5.

Specimen	**Turn-on Field, to draw J = 10 µA/cm^2**	**Threshold Field, to draw J = 100 µA/cm^2**
Specimen A	**9 V/µm**	**11 V/µm**
Specimen B	**7.5 V/µm**	**9.9 V/µm**
Specimen C	**5.6 V/µm**	**7.9 V/µm**

***Table 5**: Table of Comparison*

From **Table 5**, it is seen that the FE properties of Specimen A are inferior to Specimen B. The reason for this behavior is the difference in their morphology. The SEM images for Specimen A and B are shown in **Fig 4** and **Fig 5**, respectively. The SEM image of Specimen B reveals that the carbon nanoparticle matrix is quite dense in this case as compared to Specimen A. Moreover careful observation shows that the number of carbon nanoparticles embedded in an individual matrix is higher in Specimen B, which means more number of emitters are available.

The FE properties of Specimen C are far superior to those of Specimen A and B. This is because in sample C the effective electron emission takes place from both, the carbon nanoparticles and graphene. The atomically sharp edge of the graphene sheet can act as an additional emission site and hence the turn-on field is observed to decrease. Moreover the dispensed graphene sheets would be crumpled on a rough morphology increasing the number of favorable emitting points. The FE properties of carbon films can thus be tuned further by forming a composite or heterostructure. It will be interesting to examine *in situ* (in process) formation of rough and conducting carbon based nanocomposite films by the process discussed herein.

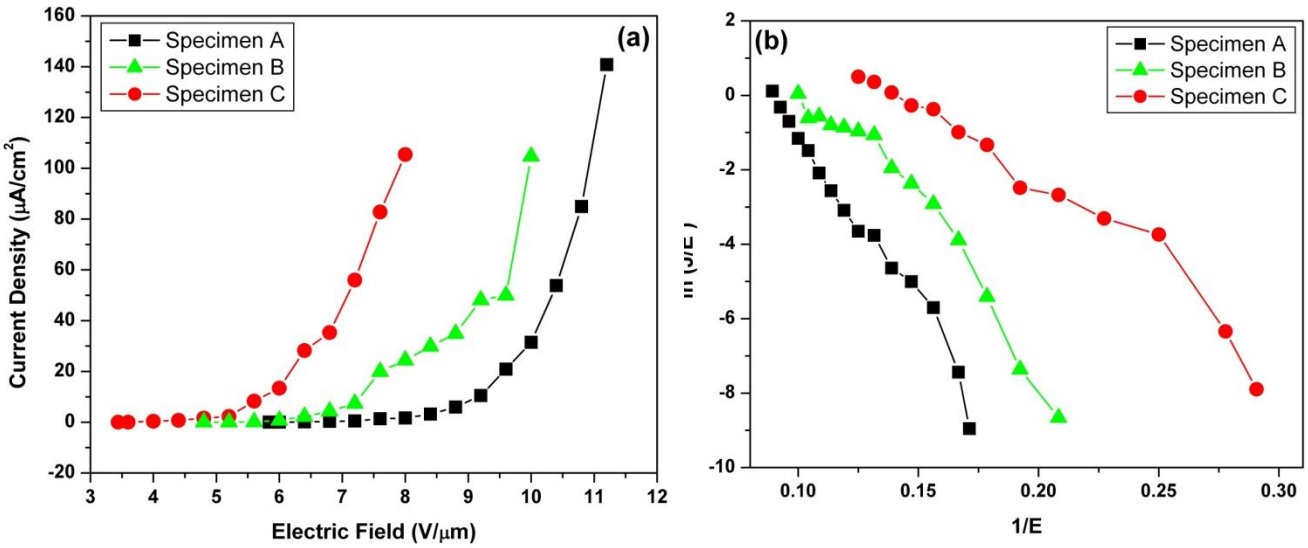

Figure S8. *Field emission Characteristics (a) Current density-applied electric field (J-E) characteristics. (b) Corresponding Fowler-Nordheim (F-N) plot.*

The Fowler-Nordheim (F-N) plot derived from the observed JE characteristic is shown in **Fig. S8** (b). The F-N plot shows an overall linear behavior with decrease in the slope (non-linearity) at very high applied field range. Such type of F-N plot exhibiting tendency toward nonlinearity at very high applied field has been reported and discussed in our previous work [4].

References:

a. S. Wu, *J. Adhesion* 1973, **5**, 39-55.

b. J. Chen, K. Li, Y. Luo, X. Guo, D. Li, M. Deng, S. Huang, Q. Meng, *Carbon* 2009, **47**, 2704 –2708.

c. W. Milne, K. Teo, G. Amaratunga, P. Legagneux, L. Gangloff, J. Schnell, V. Semet, V. Thien Binh, O. Groening, *Journal of Materials Chemistry* 2004, **14**, 933-943.

d. Z. Wu, S. Pei, W. Ren, D. Tang, L. Gao, B. Liu, F. Li, C. Liu, H. Cheng, *Advanced Materials* 2009, **21**, 1756-1760.

e. W. Kang, J. Davidson, Y. Wong, K. Holmes, *Diamond and Related Materials* 2004, **13**, 975-981

f. D. Shinde, P. Chavan, S. Sen, D. Joag, M. More, S. Gadkari, S. Gupta, *ACS Appl. Mater. Interfaces* 2011, **3**, 4730–4735